

Water-Soluble Organometallic Compounds. 6.¹ Synthesis, Spectral Properties, and Crystal Structures of Complexes of 1,3,5-Triaza-7-phosphaadamantane with Group 10 Metals

Donald J. Darensbourg,^{*,†} Tara J. Decuir, Nicole White Stafford, Jeffrey B. Robertson, Jennifer D. Draper, and Joseph H. Reibenspies

Department of Chemistry, Texas A&M University, College Station, Texas 77843

Agnes Kathó*

Institute of Physical Chemistry, Kossuth Lajos University, Debrecen 10, P.O. Box 7, H-4010 Hungary

Ferenc Joó

Institute of Physical Chemistry, Kossuth Lajos University and Hungarian Academy of Sciences, Research Group on Homogeneous Catalysis, Debrecen 10, P.O. Box 7, H-4010 Hungary

Received February 27, 1997[⊗]

The syntheses of a variety of group 10 metal complexes of the water-soluble phosphine triazaphosphaadamantane (PTA) are described. Treatment of Ni(NO₃)₂ with NaNO₂ and PTA provides the nitrosyl complex [Ni(NO)(PTA)₃]NO₃ (**1**). Complex **1** is soluble in water, DMSO, and CH₃CN but insoluble in THF, acetone, or hydrocarbons. X-ray crystallography shows the nitrosyl ligand to be coordinated in a near linear mode (\angle Ni–N–O = 171.5(4)°) with a Ni–N bond length of 1.653(4) Å. Concordantly, the ν (NO) vibration in H₂O occurs at 1830 cm⁻¹. The series of zerovalent M(PTA)₄ (M = Ni, Pd, Pt) complexes, **2**, **3**, and **6** have been prepared in good yields by several procedures: (i) the ligand exchange reaction of Ni(cod)₂ with PTA; (ii) the reduction of PdCl₂ or PtCl₂ with hydrazine in the presence of PTA; and (iii) the ligand exchange reaction of Pt(PPh₃)₄ with PTA. All three derivatives are very water soluble (0.30 M) and resistant to PTA dissociation in solution at ambient temperature. Complexes **2**, **3**, and **6** can be crystallized from 0.10 M HCl to afford the nitrogen-protonated derivatives, [M(PTAH)₄]Cl₄. These salts were characterized by X-ray crystallography and shown to exist as slightly distorted tetrahedra with one nitrogen atom of each PTA ligand protonated. The M–P bond lengths are shorter than those found in related derivatives containing poorer electron-donating and/or sterically more encumbering phosphine ligands. The *cis*-MCl₂(PTA)₂ (M = Pd and Pt) derivatives, **4** and **7**, were obtained by the metathesis reaction of (NH₄)₂PdCl₄ or K₂PtCl₄ with PTA in refluxing ethanol. When the palladium reaction was carried out in a large excess of PTA, formation of the zerovalent Pd(PTA)₄ complex occurred via the intermediacy of the [Pd(PTA)₃Cl]⁺ cation as indicated by ³¹P NMR and mass spectrometry. The X-ray structures of the Pd(II) and Pt(II) derivatives, *cis*-PdCl₂(PTA)₂ and [*cis*-PtCl₂(PTAH)₂]Cl₂, revealed these to exist as slightly distorted square planar complexes where the P–M–P angles are expanded to 94.4°. The platinum derivative, which contains the nitrogen protonated PTA ligands, displays an extensive array of hydrogen bonding and electrostatic interactions involving water, PTA, and HCl.

Introduction

The separation of expensive transition metal catalysts from substrate(s) and product(s) mandatory for industrial applications of homogeneous catalysis has led to the development of several concepts for low-cost catalyst recovery. These include the use of multiphase reaction systems.² Prominent among these currently receiving wide attention is liquid/liquid biphasic systems, where the two solvents have limited miscibility.³ One of the most common of these processes is one in which the catalyst is soluble in water while the substrate(s)/product(s) are

soluble only in the organic phase, hence providing a feasible separation process. Organotransition metal complexes can be solubilized in an aqueous medium by utilizing a variety of tertiary phosphines, which themselves are made water-soluble by virtue of attaching hydrophilic polar (ionic) groups such as sulfonate, carboxylate, phosphonate, or ammonium functionalities.⁴ Recent advances in the use of nonionic ligands such as *tris*(hydroxymethyl)phosphine, P(CH₂OH)₃, and related diphosphine and triphosphine derivatives⁵ and 1,3,5-triaza-7-phosphaadamantane have been made.⁶

[†] Correspondance may be addressed *via* given address or e-mail: djdarens@chemvx.tamu.edu.

[⊗] Abstract published in *Advance ACS Abstracts*, August 15, 1997.

- (1) Darensbourg, D. J.; Stafford, N. W.; Joó, F.; Reibenspies, J. H. *J. Organomet. Chem.* **1995**, 488, 99.
 (2) (a) Chaloner, P. A.; Esteruelas, M. A.; Joó, F.; Oro, L. A. *Homogeneous Hydrogenation (Catalysis by Metal Complexes)*; Kluwer Academic: Dordrecht, The Netherlands, 1994; Chapter 6, p 241. (b) Arhancet, J. P.; Davis, M. E.; Merola, J. S.; Hanson, B. E. *J. Catal.* **1990**, 121, 237. (c) Beller, M.; Cornils, B.; Frohning, C. D.; Kohlpaintner, C. W. *J. Mol. Catal. A.* **1995**, 109, 17.

- (3) (a) Herrmann, W. A.; Kohlpaintner, C. W. *Angew. Chem.* **1993**, 105, 1588; *Angew. Chem., Int. Ed. Engl.* **1993**, 32, 1524. (b) Horváth, I. T.; Rábai, J. *Science* **1994**, 226, 72.
 (4) (a) Joó, F.; Tóth, Z. *J. Mol. Catal.* **1980**, 8, 369. (b) Herd, O.; Langhans, K. P.; Stelzer, O. *Angew. Chem., Int. Ed. Engl.* **1993**, 32, 1058. (c) Schull, T. L.; Fettingner, J. C.; Knight, D. A. *Inorg. Chem.* **1996**, 35, 6717. (d) Amrani, Y.; Lecompte, L.; Sinou, D. *Organometallics* **1989**, 8, 542. (e) Ahrland, S.; Chatt, J.; Davies, N. R.; Williams, A. A. *J. Chem. Soc.* **1958**, 276. (f) Tóth, I.; Hanson, B. E.; Davis, M. E. *Organometallics* **1990**, 9, 675. (g) Ravinder, V.; Hemling, H.; Schumann, H.; Blum, J. *Synth. Commun.* **1992**, 22, 841.

Complexes of low-valent group 10 metals are some of the most important complexes used as catalyst precursors in homogeneous processes. Derivatives of all three are known to catalyze hydrogenation reactions, where the general activity follows the trend Pd > Pt > Ni.⁷ Palladium complexes find effective use as catalysts for the Heck reaction and as catalytic intermediates in a variety of cross-coupling reactions, processes which have recently been studied under aqueous conditions.^{8,9} Palladium complexes also catalyze the oxidation of alkenes (Wacker Process), as well as the carbonylation of alkenes⁷ and allylic chlorides^{4c,10} to afford aldehydes in the presence of CO. Additionally, platinum complexes are known to catalytically activate dioxygen, finding utility in the oxidation of various substrates including alcohols.⁷

With the increase in studies of homogeneous catalytic processes in aqueous solutions, it is appropriate to extend these investigations to other systems involving complexes of the group 10 metals. The water-soluble phosphine ligand, P(CH₂OH)₃, has been utilized to synthesize such metal derivatives. For example, Chatt and co-workers^{5a} have reported the synthesis of the dichloro complexes, MCl₂[P(CH₂OH)₃]₂ (M = Pd and Pt), and more recently Pringle and co-workers^{5b} have prepared and fully characterized the zero valent metal derivatives, M[P(CH₂OH)₃]₄ (M = Ni, Pd, Pt). Closely related water-soluble hydroxymethyl bis(phosphine) complexes of Pd(II) and Pt(II) have been synthesized by Katti and co-workers.^{5c} Herein we wish to describe well-characterized analogous complexes, in addition to a nitrosyl derivative, employing the water-soluble phosphine ligand 1,3,5-triaza-7-phosphaadamantane (PTA), which was first synthesized by Daigle.¹¹ Included will be the synthesis and spectroscopic characterization of [Ni(NO)(PTA)₃]-NO₃, **1**, Ni(PTA)₄, **2**, Pd(PTA)₄, **3**, *cis*-PdCl₂(PTA)₂, **4**, [PdCl(PTA)₃]Cl, **5**, Pt(PTA)₄, **6**, and *cis*-PtCl₂(PTA)₂, **7**, as well as the solid-state structures of the tetraphenylborate salt of **1**, **4**, and the protonated forms of **2**, **3**, **6**, and **7**.

Experimental Section

Methods and Materials. All manipulations were carried out under an inert atmosphere, either argon or nitrogen, unless otherwise indicated. The compounds, PdCl₂, PtCl₂, Pd(PPh₃)₄, Pt(PPh₃)₄, (NH₄)₂PdCl₄, and

K₂PtCl₄, were purchased from Strem Chemicals, Ni(NO₃)₂·6H₂O was purchased from Fischer Scientific, and NaNO₂ was purchased from Aldrich. All were used as received without further purification. Ni(COD)₂ was synthesized according to the procedure previously reported.¹² The water-soluble phosphine, 1,3,5-triaza-7-phosphaadamantane (PTA), was synthesized as described by Daigle and co-workers.¹¹ The water which was used was doubly distilled and deionized and had been purged with argon or nitrogen for at least 30 min prior to use. Deuterated solvents were purchased from Cambridge Isotopes Laboratories and used as received; the D₂O was stored in an airtight flask under argon at all times. Benzene, toluene, methanol, and ethanol were purchased from Fischer Scientific and freshly distilled from respective drying agents before each use; benzene and toluene were stored over Na/benzophenone, and methanol and ethanol were stored over Mg/I₂. Dimethyl sulfoxide was purchased from Aldrich Chemicals and used as received. Carbon monoxide was purchased from Matheson Gas Products, Inc., and used without further purification. All NMR spectra were recorded on either a Varian 200XL broadband or a Varian Unity-300 spectrometer. The ³¹P NMR data were recorded against an external reference of 85% H₃PO₄, δ = 0.0 ppm. The infrared samples were recorded on a Mattson 6021 Galaxy Series FT-IR in a 0.01 mm CaF₂ cell for water samples, 0.1 mm NaCl for other solution samples, and KBr for solid samples. Elemental analyses were carried out by Galbraith Laboratories or Canadian Microanalytical Service, Ltd. Mass spectral analyses were carried out by the Mass Spectrometry Applications Laboratory at Texas A&M University, where specific experimental methods are noted accordingly (+ESI = electrospray ionization).

Nitrosyltris(1,3,5-triaza-7-phosphaadamantane)nickel(0) Nitrate, 1. To 785 mg (5 mmol) of PTA dissolved in 20 mL of hot, absolute ethanol was added 1 mL of aqueous solution containing 291 mg (1 mmol) of Ni(NO₃)₂·6H₂O and 104 mg (1.5 mmol) of NaNO₂ under an inert atmosphere. Upon addition the solution turned deep blue (almost black) and changed to brown in color in less than 5 min. The solution was refluxed for 3 h, during which it turned dark purple and formed a pale purple precipitate. The warm solution was filtered through a sintered glass frit to afford a pale purple solid which exhibited no NO stretching frequency in its infrared spectrum. The nitrosyl complex was isolated by cooling the dark purple filtrate in the refrigerator (5 °C) overnight, yielding a dark purple, almost black, shiny crystalline solid. Yield: 36.2%. Anal. Calc for NiP₃C₁₈H₃₆N₁₁O₄: 34.75, C; 5.83, H; 24.76, N. Found: 28.02, C; 5.69, H; 21.37, N. Analysis of the product indicates the presence of a sodium nitrate impurity which coprecipitates due to its similarity in solubility with that of the nickel complex, in addition to waters of solvation. Indeed, the elemental analysis is consistent with a complex of composition [Ni(NO)(PTA)₃]-NO₃·NaNO₃·4H₂O, which requires the following (%): C, 27.75; H, 5.69; N, 21.57. Mass spectrometry (+ESI in 50:50 methanol/water) indicated the presence of Na⁺ (*m/z* = 23) and [Ni(NO)(PTA)₃]⁺ (*m/z* = 559). ³¹P NMR (D₂O): δ -48.2 ppm. IR (ν_{NO}): KBr, 1778 cm⁻¹; H₂O, 1830 cm⁻¹; DMSO 1786 cm⁻¹; CH₃CN, 1805 cm⁻¹; CH₃OH, 1809 cm⁻¹. The solubility of **1** was measured in H₂O (26 g/L), CH₃OH (7.5 g/L), CH₃CN (3.0 g/L), and DMSO (57 g/L). UV-vis (λ_{max}): H₂O, 362 nm (ε = 5.57 × 10² M⁻¹ cm⁻¹), 470 nm (ε = 8.64 × 10² M⁻¹ cm⁻¹), 542 nm (ε = 7.06 × 10² M⁻¹ cm⁻¹); DMSO, 348 nm (ε = 1.35 × 10³ M⁻¹ cm⁻¹), 376 nm (ε = 1.23 × 10³ M⁻¹ cm⁻¹), 476 nm (ε = 1.25 × 10³ M⁻¹ cm⁻¹), 550 nm (ε = 1.01 × 10³ M⁻¹ cm⁻¹); CH₃OH, 362 nm (ε = 1.97 × 10³ M⁻¹ cm⁻¹), 476 nm (ε = 2.10 × 10³ M⁻¹ cm⁻¹), 544 nm (ε = 1.76 × 10³ M⁻¹ cm⁻¹); CH₃CN, 368 nm (ε = 1.07 × 10³ M⁻¹ cm⁻¹), 476 nm (ε = 1.06 × 10³ M⁻¹ cm⁻¹), 550 nm (ε = 8.42 × 10² M⁻¹ cm⁻¹).

[Ni(NO)(PTA)₃][BPh₄]. Crystals suitable for X-ray analysis were obtained by dissolving 75 mg of **1** in 1.5 mL of methanol, followed by the addition of a concentrated solution of 100 mg of NaBPh₄ in methanol. The resulting solution was kept for 3 days at room temperature. Deep purple crystals appeared and were collected on a filter and washed with cold methanol. Anal. Calc for NiC₄₂H₅₆BN₁₀OP₃·3H₂O: 54.16, C; 6.49, H; 15.04, N; 9.98, P. Found: 54.36, C; 6.74, H; 14.75, N; 10.56, P.

- (5) (a) Chatt, J.; Leigh, G. J.; Slade, R. W. *J. Chem. Soc., Dalton Trans.* **1973**, 2021. (b) Ellis, J. W.; Harrison, K. N.; Hoye, P. A. T.; Orpen, A. G.; Pringle, P. G.; Smith, M. B. *Inorg. Chem.* **1992**, *31*, 3026. (c) Reddy, V. S.; Katti, K. V.; Barnes, C. L. *J. Chem. Soc., Dalton Trans.* **1996**, 1301. (d) Katti, K. V. *Curr. Sci.* **1996**, *70*, 219. (e) Baxley, G. T.; Miller, W. K.; Lyon, D. K.; Miller, B. E.; Niecekarz, G.F.; Weakley, T. J. R.; Tyler, D. R. *Inorg. Chem.* **1996**, *35*, 6688. (f) Herrmann, W. A.; Kellner, J.; Riepel, H. *J. Organomet. Chem.* **1990**, *389*, 103. (g) Bartik, T.; Bunn, B. B.; Bartik, B.; Hanson, B. E. *Inorg. Chem.* **1994**, *33*, 164. (h) Herring, A. M.; Steffy, B. D.; Miedander, A.; Wander, S. A.; DuBois, D. L. *Inorg. Chem.* **1995**, *34*, 1100.
- (6) (a) Darenbourg, D. J.; Joó, F.; Kannisto, M.; Kathó, Á.; Reibenspies, J. H.; Daigle, D. J. *Inorg. Chem.* **1994**, *33*, 200. (b) Darenbourg, D. J.; Joó, F.; Kannisto, M.; Kathó, Á.; Reibenspies, J. H. *Organometallics* **1992**, *11*, 1990. (c) Fackler, J. P., Jr.; Staples, R. J.; Assefa, Z. *J. Chem. Soc., Chem. Comm.* **1994**, 431. (d) Assefa, Z.; McBurnett, B. G.; Staples, R. J.; Fackler, J. P., Jr. *Inorg. Chem.* **1995**, *34*, 75. (e) Joó, F.; Nádasdi, L.; Bényei, A. C.; Darenbourg, D. J. *J. Organomet. Chem.* **1996**, *512*, 45. (f) Fisher, K. J.; Alyea, E. C.; Shahnazarian, N. *Phosphorus, Sulfur, Silicon* **1990**, *48*, 37.
- (7) (a) James, B. R. *Homogeneous Hydrogenation*; Wiley: New York, 1973. (b) Chaloner, P. A. *Handbook of Coordination Catalysis in Organic Chemistry*; Butterworths: London, 1986.
- (8) Kiji, J.; Okano, T.; Hasegawa, T. *J. Mol. Catal. A* **1995**, *73*.
- (9) Wallow, T. I.; Goodson, F. E.; Novak, B. M. *Organometallics* **1996**, *15*, 3708.
- (10) (a) Okano, T.; Hayashi, T.; Kiji, J. *Bull. Chem. Soc. Jpn.* **1994**, *67*, 2339. (b) Okano, T.; Moriyama, Y.; Konishi, H.; Kiji, J. *Chem. Lett.* **1986**, 1463.
- (11) Daigle, D. J.; Pepperman, A. B., Jr.; Vail, S. L. *Heterocycl. Chem.* **1974**, *11*, 407.

- (12) Ittel, S. D. *Inorg. Synth.* **1990**, *28*, 98.

Tetrakis(1,3,5-triaza-7-phosphaadamantane)nickel(0), 2. A 0.500 g (1.81 mmol) amount of Ni(COD)₂ was placed in a flame-dried 100 mL Schlenk flask and was then dissolved in 45 mL of toluene. The resulting solution was filtered to remove any metallic nickel. A solution of 1.16 g (7.56 mmol) of PTA in 25 mL of methanol was then cannulated over to the Ni(COD)₂ solution. A white precipitate formed immediately as the yellow color of the Ni(COD)₂ solution faded. The resulting mixture was allowed to stir for an additional 1/2 h and was then filtered onto a sintered glass frit and allowed to dry overnight *via* vacuum. The white powder was isolated to give 1.02 g (82.3% yield). Anal. Calc for NiP₄N₁₂C₂₄H₄₈·2H₂O: 39.88, C; 7.19, H; 23.24, N. Found: 39.09, C; 6.82, H; 21.99, N. ³¹P NMR (δ): D₂O, -45.7 ppm;¹³ 0.1 M HCl/D₂O, -41.9 ppm. ¹H NMR (D₂O): δ 3.76 ppm (singlet), 4.75 ppm (quartet).

Ni(PTAH)₄Cl₄·H₂O. Crystals of the protonated form of **2** were grown by dissolving 80 mg (0.12 mmol) of **2** in 5 mL of 0.1 M HCl. This was then divided into two aliquots, each of which was layered with 2.5 mL of methanol under an inert atmosphere. The solutions were allowed to diffuse overnight, during which time small clear crystals appeared.

Tetrakis(1,3,5-triaza-7-phosphaadamantane)palladium(0), 3. This method follows that described by Coulson for the synthesis of Pd(PPh₃)₄.¹⁴ To a 100 mL Schlenk flask containing 0.88 g (4.9 mmol) of PdCl₂ and 3.1 g (20 mmol) of PTA was added 40 mL of deaerated DMSO. The solution was heated to 130 °C, upon which the solids dissolved. Subsequently, 1 mL of hydrazine monohydrate was added *via* syringe, upon which the solution turned dark brown. The solution was allowed to cool to room temperature, followed by the addition of absolute ethanol. The resulting solution was coffee brown and contained a tan precipitate. The solution was filtered through a sintered glass frit, and the solid was washed several times with 5 mL aliquots of dry benzene and then dried overnight under vacuum (yield 79%). Anal. Calc for PdP₄C₂₄H₄₈N₁₂·HCl: 37.36, C; 6.41, H; 21.79, N. Found: 36.69, C; 6.51, H; 21.67, N. ³¹P NMR (δ): D₂O, -58.7 ppm; 0.1 M HCl/D₂O, -54.2 ppm. An alternative synthetic route to this complex has previously been reported.¹³ However, its ³¹P NMR signal was observed at -10.8 ppm with coupling constants of ¹J(P-C) of 50.3 Hz and ³J(P-C) of 9.3 Hz.

Pd(PTAH)₄Cl₄·H₂O. Crystals of the protonated form of **3** were grown by dissolving 51 mg (0.69 mmol) of **3** in 5 mL of 0.1 M HCl. The sample was divided into four, 1 mL aliquots, and each was layered with 2 mL of dry methanol under an argon atmosphere. The solutions were allowed to slowly diffuse at room temperature for 3 days, during which time small pale yellow crystals appeared. ³¹P NMR (D₂O): δ -54.2 ppm.

cis-Dichlorobis(1,3,5-triaza-7-phosphaadamantane)palladium(II), 4. A 142 mg (0.5 mmol) amount of (NH₄)₂PdCl₄ was dissolved in air in 10 mL of 95% ethanol in a 50 mL Schlenk flask, which was evacuated and filled with an argon atmosphere. The solution was then heated to 60 °C. To the resulting light brown solution, containing residual undissolved [PdCl₄]²⁻, was added 160 mg (1 mmol, 2 equiv) of PTA dissolved in 1 mL of warm ethanol. The color of the solution changed immediately to greenish-yellow, and a yellow precipitate formed within 1 min. Heating was continued for 2 h. Upon cooling to room temperature, the solution was filtered through a sintered glass frit, and the solid was subsequently washed with 5 mL aliquots of dry diethyl ether. The greenish-yellow solid was dried overnight *via* vacuum. Yield: 83% based on (NH₄)₂PdCl₄. Anal. Calc for PdCl₂P₂C₁₂H₂₄N₆·HCl: 27.28, C; 4.78, H; 15.91, Cl. Found: 27.03, C; 4.80, H; 15.64, Cl. ³¹P NMR (D₂O): δ -23.2 ppm (s).

cis-PdCl₂(PTA)₂·6H₂O. Crystals of **4** were obtained by dissolving 80 mg (0.12 mmol) of **4** in 3 mL of 0.1 M HCl. This solution was divided into 1 mL aliquots in small test tubes fitted with septa, and then each was layered with 2 mL of dry methanol. Bright yellow

needles suitable for X-ray analysis grew overnight. Anal. Calc for PdP₂C₁₂H₂₄N₆Cl₂·6H₂O: 24.08, C; 4.05, H. Found: 24.31, C; 4.87, H. ³¹P NMR (D₂O): δ -21 ppm (s).

Chlorotris(1,3,5-triaza-7-phosphaadamantane)palladium(II) Chloride, 5. A 150 mg (0.53 mmol) amount of (NH₄)₂PdCl₄ was dissolved in air in 10 mL of 95% ethanol in a 50 mL Schlenk flask. The flask was then evacuated and subsequently filled with an argon atmosphere; the solution was then heated to 60 °C. To the resulting light brown solution, containing residual undissolved [PdCl₄]²⁻, was added 415 mg (2.6 mmol, 5 equiv) of PTA. The solution immediately turned golden yellow. Heating was continued for 3 h, during which time the solution became bright yellow and a precipitate formed. After cooling the solution to room temperature, it was filtered through a sintered glass frit. The resulting bright yellow solid was washed with 5 mL aliquots of dry diethyl ether and dried overnight *in vacuo*. Yield: 72.9% based on (NH₄)₂PdCl₄. Anal. Calc for PdP₃C₁₈H₃₆N₉Cl₂: 33.32, C; 5.59, H; 10.93, Cl. Found: 31.95, C; 5.88, H; 10.56, Cl. ³¹P NMR (D₂O): δ -25 ppm (s) and -43.6 ppm, both very broad signals. Mass spectral analysis (+ESI in 50/50 H₂O/MeOH) indicated the presence of two species, the major component at *m/z* 612 ([Pd(PN₃C₆H₁₂)₃Cl]⁺) and the other at *m/z* 456 ([Pd(PN₃C₆H₁₂)₂Cl]⁺).

Tetrakis(1,3,5-triaza-7-phosphaadamantane)platinum(0), 6. Method A. This method follows that described by Tolman and co-workers for the synthesis of Pt(PPh₃)₄.¹⁵ To a 100 mL Schlenk flask containing 750 mg (2.8 mmol) PtCl₂ and 1.8 g (11.4 mmol) of PTA was added 50 mL of deaerated DMSO. The solution was then heated to 140 °C, where at approximately 60 °C the solution turned dark yellow in color. To this was added 0.6 mL (12.3 mmol) of hydrazine monohydrate *via* syringe, upon which N₂ evolved and a white precipitate formed. The solution was then quickly cooled to approximately 100 °C in an ice bath and then allowed to cool to room temperature slowly. The solution was subsequently filtered through a sintered glass frit, and the solid was washed several times with 5 mL aliquots of diethyl ether and dried overnight under vacuum (yield 67%). Anal. Calc for PtP₄C₂₄H₄₈N₁₂: 35.00, C; 5.87, H; 20.40, N. Found: 34.21, C; 5.99, H; 20.34, N. ³¹P NMR (δ): (D₂O) -74.5 ppm with Pt satellites, *J*_{Pt-P} = 3590 Hz; 0.1 M HCl/D₂O, -69.1 ppm, *J*_{Pt-P} = 3704 Hz.

Method B. This method involves a phosphine exchange process. To a 25 mL Schlenk flask containing 120 mg (0.75 mmol) of PTA and 110 mg (0.084 mmol) of Pt(PPh₃)₄ was added 10 mL of dry methanol. The solution was heated for 20 h at 50 °C and then cooled to room temperature. The solvent was removed *via* vacuum. The solid was washed with hexanes to remove any PPh₃ and dried under vacuum. ³¹P NMR (D₂O): δ -74.2 ppm, *J*_{Pt-P} = 3590 Hz; δ -2.3 ppm (PTA-oxide).

Pt(PTAH)₄Cl₄. Crystals were grown by dissolving 51 mg (0.62 mmol) of **6** in 5 mL of 0.1 M HCl. The sample was divided into four, 1 mL aliquots, and each was layered with 2 mL of dry methanol under an argon atmosphere. The solutions were allowed to slowly diffuse at room temperature for 3 days, during which small colorless crystals appeared. ³¹P NMR (D₂O): δ -69.1 ppm, *J*_{Pt-P} = 3704 Hz. Anal. Calc for PtP₄C₂₄H₅₂N₁₂Cl₄·H₂O: 14.36, Cl. Found: 14.75, Cl.

cis-Dichlorobis(1,3,5-triaza-7-phosphaadamantane)platinum(II), 7. A solution of 716 mg (1.7 mmol) of potassium tetrachloroplatinate(II) in 10 mL deaerated water was added dropwise to a boiling solution of 980 mg (6.4 mmol, 3.6 equiv) of PTA in 12 mL of 95% ethanol; the resulting solution was milky orange in appearance. The solution was kept at 60 °C for 2 h. The solvent was then removed *in vacuo*. The residual yellow solid was washed several times with ethanol and diethyl ether until an off-white powder was observed. The precipitate was collected by filtration and dried *via* vacuum (yield 52%). ¹H NMR: broad singlets at 4.9 and 4.7 ppm. ³¹P NMR: -51 ppm, with platinum satellites, *J*_{Pt-P} = 3350 Hz. Anal. Calc for PtCl₂P₂C₁₂H₂₄N₆: C, 24.84; H, 4.16. Found: C, 24.86; H, 4.63.

cis-[PtCl₂(PTAH)₂]Cl₂. Colorless crystals of the protonated form of **7** were obtained from a 0.1 M HCl solution and characterized by X-ray diffraction. Anal. Calc for PtCl₄P₂C₁₂H₂₆N₆·2H₂O: C, 20.91; H, 4.39; N, 12.19; Cl, 20.57. Found: C, 20.02; H, 4.60; N, 11.61; Cl, 20.29.

X-ray Structural Determination of 1-4, 6, and 7. Crystal data and details of data collection are given in Table 1. A dark purple plate of **1**, a colorless needle of **2**, a pale yellow plate of **3**, a yellow needle

(13) Cermak and co-workers have reported a similar synthesis of this complex, where the ³¹P NMR signal was observed at -46.5 ppm with coupling constants of ¹J(P-C) of 53.3 Hz and ³J(P-C) of 8.8 Hz. Cermak, J.; Kvalcova, M.; Blechta, V. *Abs. ISH C-10*; Princeton, NJ, 1996; p B54.

(14) Coulson, D. R. *Inorg. Synth.* 1972, 13, 121.

(15) Tolman, C. A.; Seidel, W. C.; Gerlach, D. H. *J. Am. Chem. Soc.* 1972, 94, 2669.

Table 1. Crystallographic Data for Complexes **1a–4**, **6**, and **7**

	1a	2	3
empirical formula	C ₄₂ H ₆₂ N _{10.50} NiO ₂ P ₃ B	C ₂₄ H ₆₂ Cl ₄ N ₁₂ NiO ₅ P ₄	C ₄₈ H _{114.67} Cl ₈ N ₂₄ O _{5.34} P ₈ Pd ₂
fw	933.55	923.25	1857.82
space group	triclinic, <i>P</i> $\bar{1}$	tetragonal, <i>I41/a</i>	monoclinic, <i>C2/c</i>
<i>V</i> (Å ³)	2276.9(9)	3974.5	3945(2)
<i>Z</i>	2	4	2
<i>D</i> _{calc} (g cm ^{−3})	1.361	1.543	1.564
<i>a</i> (Å)	10.760(2)	12.333(2)	13.813(3)
<i>b</i> (Å)	12.589(3)	12.333(2)	21.578(6)
<i>c</i> (Å)	17.855(4)	26.132(6)	14.425(4)
α (deg)	73.45(3)		
β (deg)	81.37(3)		113.43(2)
γ (deg)	81.27(3)		
<i>T</i> (K)	293(2)	193(2)	163(2)
μ (Mo K α) (mm ^{−1})	1.992	0.970	8.189
wavelength (Å)	1.541 78	0.710 73	1.541 78
<i>R</i> _F (%) ^a	5.61	6.83	6.30
<i>R</i> _{wF} (%) ^a	14.57	10.58	14.16

	4	6	7
empirical formula	C ₁₂ H ₃₆ Cl ₂ N ₆ O ₆ P ₂ Pd	C ₂₄ H ₅₆ Cl ₄ N ₁₂ O ₂ P ₄ Pt	C ₁₂ H ₃₀ N ₆ O ₂ P ₂ Cl ₄ Pt
fw	599.74	1005.58	689.3
space group	monoclinic, <i>P2₁/m</i>	tetragonal, <i>I4₁/a</i>	monoclinic, <i>C2/c</i> (55)
<i>V</i> (Å ³)	1222.3 (12)	4018 (3)	2332 (3)
<i>Z</i>	2	4	4
<i>D</i> _{calc} (g cm ^{−3})	1.629	1.662	1.963
<i>a</i> (Å)	12.755 (7)	12.466 (3)	10.406 (8)
<i>b</i> (Å)	7.103 (3)	12.466 (3)	24.22 (2)
<i>c</i> (Å)	14.877 (11)	25.85 (2)	9.264 (4)
α (deg)			
β (deg)	114.93 (4)		92.69 (5)
γ (deg)			
<i>T</i> (K)	293 (2)	193 (2)	193 (2)
μ (Mo K α) (mm ^{−1})	1.147	3.958	6.697
wavelength (Å)	0.710 73	0.710 73	0.710 73
<i>R</i> _F (%) ^a	12.28	7.01	7.79
<i>R</i> _{wF} (%) ^a	32.49	16.63	7.68

$$^a R_F = \frac{\sum |F_o| - |F_c|}{\sum F_o} \text{ and } R_{wF} = \left\{ \frac{\sum w(F_o - F_c)^2}{\sum wF_o^2} \right\}^{1/2}.$$

of **4**, a colorless block of **6**, and a colorless plate of **7** were mounted on glass fibers with epoxy cement at room temperature and cooled in a liquid nitrogen cold stream. Preliminary examination and data collection were performed on a Rigaku AFC5R X-ray diffractometer (Cu K α , $\lambda = 1.541 78$ Å radiation) for **1** and **3**, a Nicolet R3m/v X-ray diffractometer (Mo K α , $\lambda = 0.710 73$ Å radiation) for **7**, and a Siemens P4 diffractometer for **2**, **4**, and **6** (also Mo K α , $\lambda = 0.710 73$ Å radiation). Cell parameters were calculated from the least-squares fitting of the setting angles for 24 reflections. ω scans for several intense reflections indicated acceptable crystal quality. Data were collected for $4.0^\circ \leq 2\theta \leq 50^\circ$. Three control reflections, collected every 97 reflections, showed no significant trends. Background measurements by stationary-crystal and stationary-counter techniques were taken at the beginning and end of each scan for half the total scan time. Lorentz and polarization corrections were applied to 7146 reflections for **1**, 1768 for **2**, 3088 for **3**, 2131 for **4**, 1917 for **6**, and 1915 for **7**. A semiempirical absorption correction was applied to **6** and **7**. A total of 6789 unique reflections for **1**, 1621 for **2**, 2952 for **3**, 2035 for **4**, 1755 for **6**, and 1899 for **7**, with $|I| \geq 2.0\sigma(I)$, were used in further calculations. All six structures were solved by direct methods [SHELXS program package, Sheldrick (1993)]. Full-matrix least-squares anisotropic refinement for all non-hydrogen atoms yielded $R = 5.61$, $R_w = 14.57$, and $S = 1.049$ for **1**; $R = 6.83$, $R_w = 10.58$, and $S = 1.001$ for **2**; $R = 6.30$, $R_w = 10.79$, and $S = 1.049$ for **3**; $R = 12.28$, $R_w = 32.49$, and $S = 1.106$ for **4**; $R = 7.01$, $R_w = 16.63$, and $S = 1.035$ for **6**; and $R = 7.01$, $R_w = 16.63$, and $S = 1.035$ for **7**. Hydrogen atoms were placed in idealized positions with isotropic thermal parameters fixed at 0.08. Neutral-atom scattering factors and anomalous scattering correction terms were taken from *International Tables for X-ray Crystallography*.

Results and Discussion

Synthesis and Solution Characterization of [Ni(NO)₃(PTA)₃]NO₃, **1.** The reaction of Ni(NO₃)₂·6H₂O (1.0 equiv) with

NaNO₂ (1.5 equiv) and PTA (5.0 equiv) in ethanol and subsequent workup provided dark purple, almost black, crystalline product **1**. The ³¹P NMR (D₂O) spectrum of **1** exhibited a sharp singlet at −48.2 ppm; however when the spectrum was taken in 0.1 M HNO₃/D₂O, the solution fades from dark purple to colorless, and the only phosphorus signals present were at 42.7 ppm, −2.5 ppm (O=PTA), and −90.5 ppm (PTAH⁺). Integrations indicated a ratio of 1:7.5:13, respectively for the three phosphorus-containing species in solution. Hence, it was concluded that complex **1** is unstable in acidic solutions, even upon addition of exactly 1 equiv of acid per PTA ligand. Complex **1** was observed to be soluble in water and DMSO, having measured solubilities of 26 and 57 g/L, respectively, as well as in acetonitrile (3.0 g/L) and methanol (7.5 g/L), but was found to be insoluble in THF, acetone, and hexanes.

The $\nu(\text{NO})$ vibration of complex **1** was observed at 1778 cm^{−1} in the solid state (KBr), and was shifted to higher frequencies in solution due to solvent interactions with either the PTA ligands and/or the nitrosyl moiety.¹⁶ The observed shifts, $\Delta(\nu(\text{NO})_{\text{solution}} - 1778 \text{ cm}^{-1})$, were found to be quite sensitive to the nature of the solvent, with $\Delta\nu(\text{NO})$ being 52 cm^{−1} (water), 31 cm^{−1} (methanol), 27 cm^{−1} (acetonitrile), and 8 cm^{−1} (DMSO), respectively. Although there are *other water-soluble, well-characterized, metal nitrosyls in the literature*,¹⁷ their $\nu(\text{NO})$ vibrational modes were not reported in aqueous solution.

(16) (a) Richter-Addo, G. B.; Legdzins, P. *Metal Nitrosyls*; Oxford University Press: Oxford, U.K., 1992. (b) Hunter, A. D.; Legdzins, P. *Organometallics*, **1986**, *5*, 1001.

(17) (a) Hoshino, M.; Ozawa, K.; Seki, H.; Ford, P. C. *J. Am. Chem. Soc.* **1993**, *115*, 9568. (b) Svetlanova-Larsen, A.; Zoch, C. R.; Hubbard, J. L. *Organometallics* **1996**, *15*, 3076.

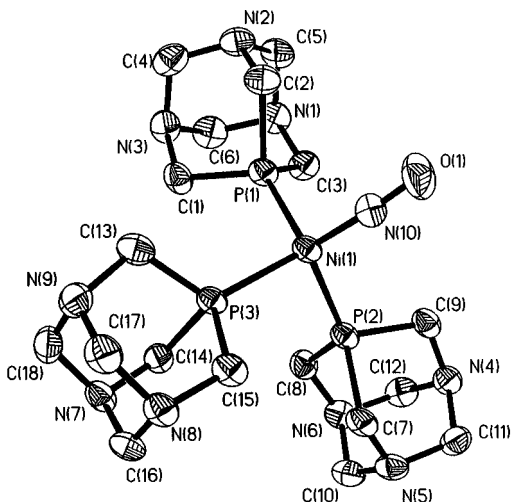


Figure 1. Thermal ellipsoid drawing of the cation of $[\text{Ni}(\text{NO})(\text{PTA})_3][\text{BPh}_4]$, **1a**, with atom-numbering scheme. Hydrogen atoms have been eliminated for simplicity.

Table 2. Selected Bond Distances (Å)^a and Bond Angles (deg)^a for $[\text{Ni}(\text{NO})(\text{PTA})_3]\text{BPh}_4$, **1a**

Ni(1)–N(10)	1.653(4)	N(1)–C(6)	1.460(5)
Ni(1)–P(1)	2.2081(14)	N(2)–C(2)	1.464(6)
Ni(1)–P(2)	2.252(2)	N(2)–C(4)	1.456(7)
Ni(1)–P(3)	2.2252(14)	N(2)–C(5)	1.454(6)
O(1)–N(10)	1.159(5)	N(3)–C(1)	1.481(6)
N(1)–C(3)	1.455(6)	N(3)–C(4)	1.472(6)
N(1)–C(5)	1.461(6)	N(3)–C(6)	1.477(6)
O(1)–N(10)–Ni(1)	171.5(4)	C(5)–N(1)–C(6)	108.2(4)
N(10)–Ni(1)–P(1)	108.41(14)	C(2)–N(2)–C(4)	111.4(4)
N(10)–Ni(1)–P(2)	112.95(13)	C(2)–N(2)–C(5)	111.8(4)
N(10)–Ni(1)–P(3)	121.96(13)	C(4)–N(2)–C(5)	109.0(4)
P(1)–Ni(1)–P(2)	107.80(6)	C(4)–N(3)–C(1)	110.8(4)
P(1)–Ni(1)–P(3)	100.99(5)	C(4)–N(3)–C(6)	108.3(4)
C(3)–N(1)–C(5)	110.6(4)	C(6)–N(3)–C(1)	110.5(4)
C(3)–N(1)–C(6)	111.4(4)		

^a Estimated standard deviations are given in parentheses.

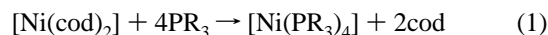
The electronic spectra of complex **1** in these solvents show only slight differences, i.e., peak patterns remain constant, with the increase in ϵ being no greater than a factor of two.

Solid-State Structure of $[\text{Ni}(\text{NO})(\text{PTA})_3][\text{BPh}_4]$. Crystals of **1** were obtained by ion-exchange from NO_3^- to BPh_4^- , a more bulky counterion, affording larger and X-ray quality crystals. Crystallographic data and data collection parameters for **1** determined at 293 K may be found in Table 1. An ORTEP view of **1** is shown in Figure 1 along with the atom-numbering scheme. The pertinent bond distances and bond angles are listed in Table 2.

The nitrosyl complex **1** exists as a slightly distorted tetrahedron, and is quite similar structurally to the analogous $[\text{Ni}(\text{NO})(\text{PMe}_3)]\text{PF}_6$.¹⁸ The Ni–N bond distance in **1a** is 1.653(4) Å, and the corresponding metric parameter in the PMe_3 complex is 1.645(5) Å.¹⁸ These Ni–N bond distances are within the range of observed values of other Ni–nitrosyl complexes which have an average of 1.69 Å.^{18,19} The nitrosyl ligand is

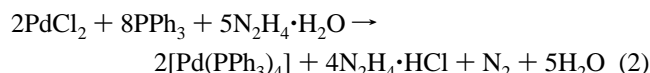
coordinated in a near 'linear' mode, having a Ni–N–O bond angle of 171.5(4)°, whereas that of the PMe_3 analog is 175.4–(5)°.¹⁸ Although the Ni–N–O bond is nearly linear, supporting the coordination as NO^+ , complex **1** does not undergo nucleophilic addition reactions characteristic of NO^+ such as the reversible addition of OH^- . Complex **1** yields a precipitate, presumably $\text{Ni}(\text{OH})_2$, upon reaction with hydroxide ions. In addition there was no color change and/or gas evolution upon addition of NH_2OH , N_2H_4 , or diamines. The average Ni–P bond distance in **1** is 2.228 Å, slightly shorter than that found in the PMe_3 complex, 2.235 Å. This slight difference in bond length can be attributed to the difference in the steric requirements of PMe_3 (Tolman cone angle, 118°)²⁰ which is somewhat larger than that of PTA (Tolman cone angle, 102°).^{6a,b} The average P–Ni–P bond angle is 104.15°, and notably the NO is slightly bent toward the plane containing P(1) and P(2), which coincidentally have the largest P–Ni–P bond angle at 107.80(6)°.

Synthesis and Solution Characterization of $\text{M}(\text{PTA})_4$ Complexes. $\text{Ni}(\text{PTA})_4$. The preferred approach for the synthesis of NiL_4 complexes, where L represents a large variety of trivalent phosphorus ligands, is depicted in eq 1.^{5b,13} By this



route the tetraligated nickel(0)/PTA complex was isolated from the ligand exchange reaction of $\text{Ni}(\text{cod})_2$ (cod = cycloocta-1,5-diene) in the presence of 4 equiv of PTA in a toluene/methanol solvent mixture. The product, $\text{Ni}(\text{PTA})_4$, precipitates out of solution as a white powder in a yield of 82.3%. Complex **2** was found to be soluble in both neutral and acidic (0.1 M HCl) aqueous solutions, having measured solubilities of 200 g/L (0.291 mol/L) and 400 g/L (0.433 mol/L), respectively. The ³¹P NMR spectrum of **2** exhibited a singlet at –45.7 ppm in D_2O which was shifted downfield to –41.9 ppm in 0.1 M HCl/ D_2O . This ³¹P NMR shift upon protonation of PTA is characteristic of the free ligand as well, which shifts from –96 ppm (D_2O) to –90 ppm (0.1 M HCl/ D_2O).

Pd(PTA)₄. The method utilized for the synthesis of $\text{Pd}(\text{PTA})_4$ was first described by Coulson for the synthesis of $\text{Pd}(\text{PPh}_3)_4$ which involves the reduction of Pd(II) by hydrazine (eq 2).¹⁴ Similarly, isolation of the zerovalent $\text{Pd}(\text{PTA})_4$, **3**,



was achieved in a yield of 79% from the reduction of PdCl_2 using hydrazine monohydrate in the presence of 4 equiv of PTA in a solution of refluxing DMSO. The ³¹P NMR spectrum of **3** in D_2O exhibits a single, sharp peak at –58.7 ppm which shifts to –54.2 ppm in 0.1 M HCl(D_2O). The solubility of **3** in water is 240 g/L (0.33 mol/L) and decreases to 120 g/L (0.16 mol/L) in 0.1 M HCl. On the other hand, the solubility of the free ligand, PTA, is 340 g/L (2.1 mol/L) in water and 350 g/L (2.2 mol/L) in 0.1M HCl.

Pt(PTA)₄. The synthesis of $\text{Pt}(\text{PTA})_4$, **6**, was accomplished by employing two different methodologies. Complex **6** was prepared by a procedure analogous to that used in the preparation of the palladium analog¹⁴ first employed by Tolman and co-workers for the synthesis of $\text{Pt}(\text{PPh}_3)_4$.¹⁵ In this manner complex **6** was prepared as an off-white solid in 67% yield. The solubility of **6** in water was determined to be 295 g/L (0.36 mol/L) and 290 g/L (0.35 mol/L) in 0.1 M HCl. The ³¹P NMR spectrum of **6** in H_2O exhibited a single resonance at –74.5

(18) Elbaze, G.; Dahan, F.; Dartiguenave, M.; Dartiguenave, Y. *Inorg. Chim. Acta* **1984**, *87*, 91.

(19) (a) Enemark, J. H. *Inorg. Chem.* **1971**, *10*, 1952. (b) Haller, K. J.; Enemark, J. H. *Inorg. Chem.* **1978**, *17*, 3552. (c) Krieger-Simonsen, J.; Elbaze, G.; Dartiguenave, M.; Feltman, R. D.; Dartiguenave, Y. *Inorg. Chem.* **1982**, *21*, 230. (d) Meiners, J. H.; Rix, C. J.; Clardy, J. C.; Verkade, J. G. *Inorg. Chem.* **1975**, *14*, 705. (e) Albricht, J. O.; Tanzella, F. L.; Verkade, J. G. *J. Coord. Chem.* **1976**, *6*, 225. (f) Berglung, D.; Meek, D. W. *Inorg. Chem.* **1978**, *17*, 1493. (g) Kaduk, J. A.; Ibers, J. A. *Isr. J. Chem.* **1976/1977**, *15*, 143.

(20) Tolman, C. A. *Chem. Rev.* **1977**, *77*, 313.

ppm with satellites due to ^{195}Pt coupling ($J_{\text{Pt-P}} = 3590$ Hz). In the presence of 0.10 M HCl, the ^{31}P signal in complex **6** shifted downfield to -69.1 ppm with a $J_{\text{Pt-P}}$ of 3704 Hz.

Alternatively, complex **6** was synthesized *via* a ligand exchange reaction, whereby an excess of PTA (8 equiv) and $\text{Pt}(\text{PPh}_3)_4$ were reacted in MeOH at 50°C for an extended period of time. However this procedure resulted in a mixture of phosphine complexes. The water-soluble portion of the reaction product displayed a ^{31}P NMR spectrum in D_2O consistent with the complex synthesized *via* the reduction of platinum chloride ($\delta = -74.2$ ppm, $J_{\text{Pt-P}} = 3590$ Hz). The other water-insoluble material appeared to be a mixture of $\text{Pt}(\text{PTA})_n(\text{PPh}_3)_{4-n}$ derivatives. That is, when the ligand exchange reaction was monitored by ^{31}P NMR in CD_3OD two sets of signals due to PTA were noted. A singlet at -71.9 ppm, having a ^{195}Pt – ^{31}P coupling constant of 3602 Hz, was observed which was assigned to complex **6**, where the peak position and coupling constant were slightly different from that previously noted due to solvent effects.²¹ The second set of peaks appears as a doublet at -75.1 ppm and has a ^{195}Pt – ^{31}P coupling constant of 3688 Hz and a ^{31}P – ^{31}P coupling constant of 38.4 Hz. This second peak was ascribed to be a mixed phosphine complex, $\text{Pt}(\text{PTA})_n(\text{PPh}_3)_{4-n}$, which is not water soluble, as indicated by its absence in the ^{31}P NMR spectrum run in D_2O . Other peaks present in the spectrum were those for the free ligands at -97 ppm (free PTA) and -6 ppm (free PPh_3).

The magnitude of $J_{^{195}\text{Pt}-^{31}\text{P}}$ observed in complex **6** (3590 Hz) can be taken as indication that the platinum PTA derivative in solution is the tetraphosphine complex of $\text{Pt}(0)$.¹⁵ That is, the ^{195}Pt – ^{31}P coupling constant in $\text{Pt}(0)$ –phosphine derivatives has been shown to be sensitive to the number of phosphine ligands coordinated to the metal center. In known $\text{Pt}(\text{PR}_3)_n$ complexes, it is generally observed that $J_{\text{Pt-P}}$ for $\text{Pt}(\text{PR}_3)_3$ derivatives is greater than 4100 Hz, whereas the corresponding values in $\text{Pt}(\text{PR}_3)_4$ species lie in the range 3500–3800 Hz.¹⁵ For example, the complexes $\text{Pt}(\text{PMe}_3)_4$ and $\text{Pt}(\text{PPh}_3)_3$ have $J_{\text{Pt-P}}$ values of 3828 and 4370 Hz, respectively.^{22c} This increase in magnitude of $J_{\text{Pt-P}}$ in $\text{Pt}(\text{PR}_3)_3$ *vs* $\text{Pt}(\text{PR}_3)_4$ complexes has been attributed to an increase in s character in the Pt-PR_3 bonds in the former complexes,^{22c} analogous to that observed in sp^2 *vs* sp^3 carbon–hydrogen bonds.

Similarly, the nature of complexes **2** and **3** in solution were demonstrated to be the tetraphosphine species, $\text{Ni}(\text{PTA})_4$ and $\text{Pd}(\text{PTA})_4$, respectively *via* ^{31}P NMR spectroscopy. Additional evidence for the existence of $\text{Pt}(\text{PTA})_4$ in solution was also obtained in this manner. That is, when the ^{31}P NMR spectra of complexes **2**, **3**, and **6** were determined in D_2O in the presence of excess PTA (up to 10 equiv) the ^{31}P resonances were unshifted, which is indicative of no significant phosphine dissociation in solution. By way of contrast several ML_4 complexes ($\text{M} = \text{Pd}, \text{Pt}$; $\text{L} = \text{PAR}_3, \text{PR}_3$) have been studied in solution and shown to readily dissociate phosphine ligands at ambient temperature.^{5b,14,15,20,22,23} Specifically, complexes containing triarylphosphines (PAR_3) or bulky trialkylphosphines undergo stepwise ligand dissociation in solution resulting in ML_3 and ML_2 as the predominant species in solution (eqs 3 and

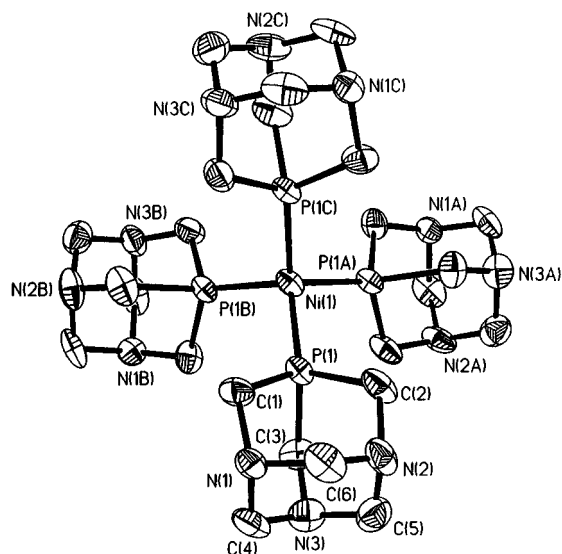


Figure 2. Thermal ellipsoid drawing of $[\text{Ni}(\text{PTAH})_4]^{4+}$, without the counterions or hydrogen atoms, with atom-numbering scheme.

4).²² In general, the metal species isolated depends strongly



on the steric requirements of the ligand (L).²³ For example, ML_2 species have been characterized for $\text{L} = \text{P}(t\text{-Bu})_3$, $\text{PPh}(t\text{-Bu})_2$, and $\text{P}(c\text{-C}_6\text{H}_{11})_3$.^{20,23} On the other hand, ML_3 species have been defined for $\text{L} = \text{P}(o\text{-o-C}_6\text{H}_4\text{CH}_3)_3$, $\text{P}(i\text{-Pr})_3$, PEt_3 , and PPh_3 .^{20,23} Although the ML_4 derivatives have been isolated for $\text{L} = \text{PEt}_3$ and PPh_3 , phosphine dissociation to provide ML_3 species in solution is substantial.^{15,22} Hence, the solution stabilities of the ML_4 ($\text{L} = \text{PTA}$) complexes can be attributed largely to the small size of the PTA ligand (cone angle $\approx 102^\circ$).²⁴ Similar solution stabilities have been noted for the group 10 metal trimethylphosphine derivatives. Indeed PTA and PMe_3 are quite comparable in both steric requirements and electronic properties.^{24,25} On the other hand, complexes of the electronically similar but sterically disparate $\text{P}(t\text{-Bu})_3$ ligand exhibit facile ligand dissociation in solution.^{22c}

Solid-State Structures of the Protonated Forms of **2, **3**, and **6**, $\text{M}(\text{PTAH})_4\text{Cl}_4$.** Small, clear to pale yellow crystals of the protonated forms of all three metal derivatives suitable for X-ray analysis were obtained by slow diffusion of methanol into a solution of **2**, **3**, or **6** in 0.10 M aqueous HCl. These complexes crystallized with varying numbers of water molecules of hydration: specifically, 5.0, 2.7, and 2.0 waters of hydration for the nickel, palladium, and platinum derivatives, respectively. Crystallographic data and data collection parameters are listed in Table 1. Thermal ellipsoid views of the respective cations are depicted in Figures 2–4, along with their atom-numbering scheme. Bond distances and bond angles of specific interest are found in Tables 3–5.

The cations, $[\text{M}(\text{PTAH})_4]^{4+}$, exist as slightly distorted tetrahedra. One nitrogen atom of each PTA ligand in the complexes is protonated as shown by the longer C–N bonds of the carbons adjacent to the protonated nitrogen. For example, in the nickel complex these C–N bond lengths have an average value of 1.507(8) Å *vs* a corresponding distance of 1.452(9) Å

(21) Sanders, J. K. M.; Hunter, B. K. *Modern NMR Spectroscopy: A Guide for Chemists*, 2nd ed.; Oxford University Press: Oxford, U.K., 1993.

(22) (a) Wilkinson, G.; Stone, G. A.; Abel, E. W. *Comprehensive Organometallic Chemistry*; Pergamon Press: New York, 1982; Vol. 6. (b) Rosenberg, B.; VanCamp, L.; Trosko, J. E.; Mansour, V. H. *Nature (London)* **1969**, 222, 385. (c) Mann, B. E.; Musco, A. *J. Chem. Soc., Dalton Trans.* **1979**, 786.

(23) Otsuka, S.; Yoshida, T.; Matsumoto, M.; Nakatsu, K. *J. Am. Chem. Soc.* **1976**, 98, 5850.

(24) DeLerno, J. R.; Trefonas, L. M.; Darensbourg, M. Y.; Majeste, R. J. *Inorg. Chem.* **1976**, 15, 816.

(25) Darensbourg, D. J.; Decuir, T. J.; Reibenspies, J. H. In *Aqueous Organometallic Chemistry and Catalysis*; Horváth, I. T., Joó, F., Eds., NATO ASI Series 3, High Technology; Kluwer: Dordrecht, The Netherlands, 1995; pp 61–77.

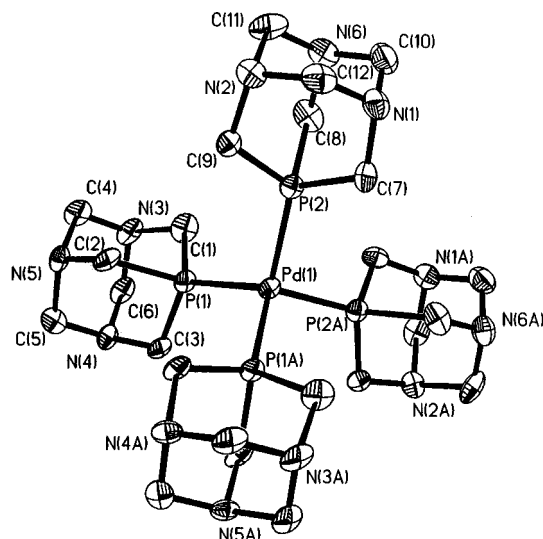


Figure 3. Thermal ellipsoid drawing of $[\text{Pd}(\text{PTAH})_4]^{4+}$, without the counterions or hydrogen atoms, with atom-numbering scheme.

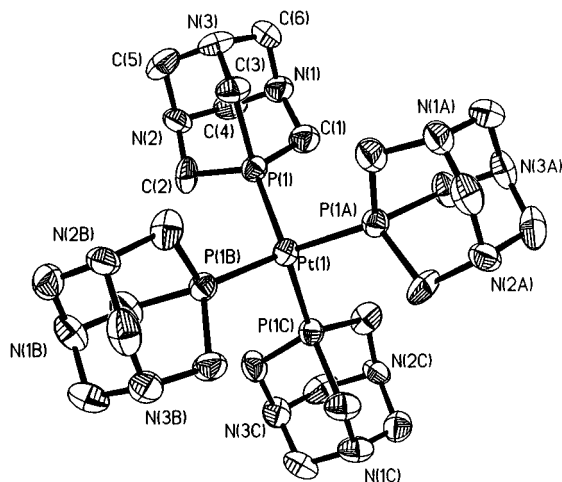


Figure 4. Thermal ellipsoid drawing of $[\text{Pt}(\text{PTAH})_4]^{4+}$, without the counterions or hydrogen atoms, with atom-numbering scheme.

Table 3. Selected Bond Distances (\AA)^a and Bond Angles (deg)^a for $[\text{Ni}(\text{PTAH})_4]\text{Cl}_4^b$

Ni(1)–P(1)	2.133(2)	N(2)–C(6)	1.445(9)
N(1)–C(1)	1.504(8)	N(2)–C(5)	1.441(9)
N(1)–C(4)	1.506(6)	N(3)–C(5)	1.459(6)
N(1)–C(6)	1.512(8)	N(3)–C(4)	1.412(9)
N(2)–C(2)	1.491(9)	N(3)–C(3)	1.464(9)
P(1)–Ni(1)–P(1) ¹	108.14(10)	P(1)–Ni(1)–P(1) ²	110.14(5)
P(1)–Ni(1)–P(2) ¹	110.14(5)	P(1)–Ni(1)–P(1) ³	108.14(10)

^a Estimated standard deviations are given in parentheses. ^b Superscripts 1–3 indicate equivalent position atoms.

to the nonprotonated nitrogen atoms. In order to detect this asymmetry in the intramolecular C–N distances, we have statistically examined in a large number of structures (37) the distributions of carbon–nitrogen bond lengths in the six-membered ring of the adamantane structure which does not contain the phosphorus atom as one of its members. We found the C–N bond lengths to be centered at 1.44 and 1.52 \AA for bonds involving N atoms nonprotonated and protonated, respectively.²⁵ In the structures reported upon herein the four chloride counterions are each associated with one nitrogen of each PTA ligand with an average $\text{N}\cdots\text{Cl}$ distance of 3.04 \AA .

The $[\text{M}(\text{PTAH})_4]^{4+}$ cations have characteristic M–P bond distances for metal(0) complexes possessing good electron-donating and sterically nonencumbering phosphine ligands. For

Table 4. Selected Bond Distances (\AA)^a and Bond Angles (deg)^a for $\text{Pd}(\text{PTAH})_4\text{Cl}_4^b$

Pd(1)–P(1)	2.203(3)	N(2)–C(11)	1.535(11)
N(1)–C(7)	1.481(11)	N(2)–C(12)	1.529(11)
N(1)–C(10)	1.455(12)	N(3)–C(1)	1.494(11)
N(1)–C(12)	1.430(12)	N(3)–C(4)	1.427(11)
N(2)–C(9)	1.501(11)	N(3)–C(6)	1.473(12)
P(1)–Pd(1)–P(1) ¹	110.01(12)	C(9)–N(2)–C(11)	111.8(6)
P(1)–Pd(1)–P(2) ¹	109.56(8)	C(9)–N(2)–C(12)	111.4(7)
P(1)–Pd(1)–P(2)	111.23(8)	C(12)–N(2)–C(11)	106.5(7)
C(12)–N(1)–C(10)	109.1(8)	C(4)–N(3)–C(1)	110.8(7)
C(10)–N(1)–C(7)	112.0(7)	C(4)–N(3)–C(6)	111.3(8)
C(12)–N(1)–C(7)	112.1(7)	C(6)–N(3)–C(1)	111.1(7)

^a Estimated standard deviations are given in parentheses. ^b Superscript 1 indicates equivalent position atoms.

Table 5. Selected Bond Distances (\AA)^a and Bond Angles (deg)^a for $\text{Pt}(\text{PTAH})_4\text{Cl}_4^b$

Pt(1)–P(1)	2.254(3)	N(2)–C(4)	1.54(2)
N(1)–C(1)	1.48(2)	N(2)–C(5)	1.53(2)
N(1)–C(4)	1.39(2)	N(3)–C(3)	1.45(2)
N(1)–C(6)	1.48(2)	N(3)–C(5)	1.43(2)
N(2)–C(2)	1.48(2)	N(3)–C(6)	1.45(2)
P(1)–Pt(1)–P(1) ⁵	108.9(2)	C(2)–N(2)–C(4)	112.7(9)
P(1)–Pt(1)–P(1) ⁶	109.75(8)	C(2)–N(2)–C(5)	111.7(9)
P(1)–Pt(1)–P(1) ⁷	109.75(8)	C(5)–N(2)–C(4)	106.2(9)
C(4)–N(1)–C(1)	113.2(11)	C(5)–N(3)–C(3)	111.5(11)
C(1)–N(1)–C(6)	109.8(10)	C(5)–N(3)–C(6)	109.5(9)
C(4)–N(1)–C(6)	110.5(10)	C(6)–N(3)–C(3)	113.0(10)

^a Estimated standard deviations are given in parentheses. ^b Superscripts 5–7 indicate equivalent position atoms.

instance, the Ni–P bond distances are 2.133(2) \AA , comparable to those found in Ni(0) phosphine derivatives.²⁶ That is, the corresponding bond lengths in $\text{Ni}(\text{PET}_3)_4$ and $\text{Ni}(\text{dppf})_2$ are 2.21^{26b} and 2.16 \AA ,^{26c} respectively. The slightly shorter Ni–P bond distance observed herein is consistent with the strong donor character and small size of the PTA ligand. Similarly, the Pt–P bond distances in the $[\text{Pt}(\text{PTAH})_4]\text{Cl}_4$ salt are 2.254(3) \AA . These are considerably shorter than those found in the less basic, larger triphenylphosphine derivative, $\text{Pt}(\text{PPh}_3)_4$, of 2.52 \AA .^{23,27} As expected, the Pd–P bond distances in the PTA derivative are 2.203(3) \AA , coincident with those of the platinum species.

Synthesis and Characterization of Pd(II) and Pt(II) PTA Complexes. *cis*- $\text{PdCl}_2(\text{PTA})_2$. The synthesis of $\text{PdCl}_2(\text{PTA})_2$ (**4**) was achieved by the metathesis reaction of $(\text{NH}_4)_2\text{PdCl}_4$ and 2 equiv of PTA in refluxing ethanol. Complex **4** was isolated as a greenish-yellow powder in 83% yield. In D_2O the ^{31}P NMR spectrum of **4** exhibited one sharp resonance at –23.2 ppm which shifted downfield to –21.0 ppm in aqueous 0.10 M HCl. Crystals of **4** were grown from a layered solution of the complex in 0.10 M HCl with methanol. Crystallographic data and data collection parameters for **4** can be found in Table 1, whereas a thermal ellipsoid drawing of **4** is depicted in Figure 5. Pertinent bond distances and angles are listed in Table 6. Although crystals of complex **4** were grown from 0.10 M aqueous HCl, the crystal chosen for analysis did not contain the expected 2 equiv of HCl. The *cis*- $\text{PdCl}_2(\text{PTA})_2$ derivative was found to possess a slightly distorted square planar geometry, with the average Cl–Pd–P (*trans*) bond angles being 176.8(2)°. Concomitantly, the P–Pd–P and Cl–Pd–Cl angles were determined to be 94.4(2) and 90.2(2)°, respectively. The mutually

(26) (a) Eishenbroich, C.; Nowotny, M.; Behrendt, A.; Massa, W.; Wocadlo, S. *Angew. Chem.* **1992**, *31*, 1343. (b) Hursthouse, M. B.; Izod, K. T.; Motewalli, M.; Thornthony, P. *Polyhedron* **1994**, *13*, 151. (c) Hartung, H.; Baumeister, U.; Walther, B.; Maschmeier, M. Z. *Anorg. Alleg. Chem.* **1989**, *578*, 177.

(27) Albano, V.; Bellon, P. L.; Scatturin V. *Chem. Commun.* **1966**, 507.

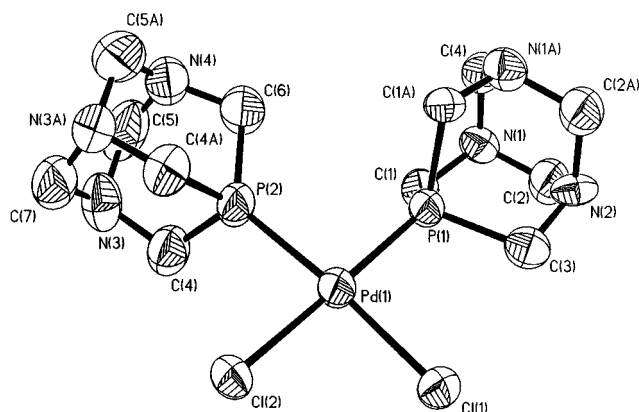


Figure 5. Thermal ellipsoid drawing of *cis*-PdCl₂(PTA)₂, **4**, with atom-numbering scheme.

Table 6. Selected Bond Distances (Å)^a and Bond Angles (deg)^a for *cis*-PdCl₂(PTA)₂

Pd(1)–P(1)	2.226(5)	Pd(1)–P(2)	2.264(6)
Pd(1)–Cl(1)	2.363(5)	Pd(1)–Cl(2)	2.360(5)
N(1)–C(1)	1.46(2)	N(2)–C(2)	1.46(2)
N(1)–C(4)	1.46(2)	N(2)–C(2A)	1.46(2)
N(1)–C(2)	1.48(2)	N(2)–C(3)	1.49(3)
N(3)–C(4)	1.48(2)	N(3)–C(7)	1.46(2)
N(3)–C(7)	1.45(2)		
P(1)–Pd(1)–P(2)	94.4(2)	P(2)–Pd(1)–Cl(2)	84.5(2)
P(1)–Pd(1)–Cl(2)	178.9(2)	P(1)–Pd(1)–Cl(1)	90.9
Cl(2)–Pd(1)–Cl(1)	90.2(2)	P(2)–Pd(1)–Cl(1)	174.7(2)

^a Estimated standard deviations are given in parentheses.

cis Pd–P and Pd–Cl bond distances were unexceptional at 2.245(6) and 2.362(5) Å.

[PdCl(PTA)₃]Cl. During an attempted preparation of the zerovalent palladium tetraphosphine derivative from the reduction of PdCl₄²⁻ in the presence of excess PTA (5 equiv) in refluxing ethanol, a bright yellow solid was isolated which was identified primarily as a mixture of Pd(II) species, PdCl₂(PTA)₂ (**4**) and [PdCl(PTA)₃]Cl (**5**), along with excess PTA. The presence of complexes **4** and **5** was suggested on the basis of the ³¹P NMR spectrum of the reaction mixture which consisted of two broad signals, one centered at –25.0 ppm due to complex **4** and the other at –43.6 ppm assigned to the [PdCl(PTA)₃] cation (*vide infra*). The broadness of these ³¹P resonances is believed to be due to ligand exchange occurring with free phosphine in solution (Figure 6). This is consistent with the observations that the ³¹P NMR spectra of isolated samples of complexes **4** and **5** in the absence of excess PTA are sharp and appear at –23.2 and –47 ppm, respectively. Corroborative evidence for the existence of the “Pd(PTA)₃” species was obtained from electrospray ionization (ESI) mass spectrometry run in a solvent mixture of 50:50 methanol/water. ESI data indicated the presence of two species, the major component having a *m/z* = 612 and the second component a *m/z* = 456. The former peak was formulated as [PdCl(PTA)₃]⁺, and the latter, as [PdCl(PTA)₂]⁺.

Upon further addition of PTA to the reaction mixture of **4** and **5**, together and individually, resulted in the formation of PTA oxide (–2.3 ppm) and Pd(PTA)₄ (–58 ppm) as well as a species with a broad ³¹P NMR resonance which shifted upfield with increasing addition of PTA (Figure 6). This latter species is ascribed to the “Pd(PTA)₃” species undergoing exchange with free PTA. After the solution was allowed to stand in the presence of excess PTA (10 equiv) for 24 h, the only detectable species in solution were Pd(PTA)₄, PTA oxide, and free PTA (Figure 7). Hence, the reaction sequence for the formation of Pd(PTA)₄ *via* the phosphine reduction of palladium(II) chloride

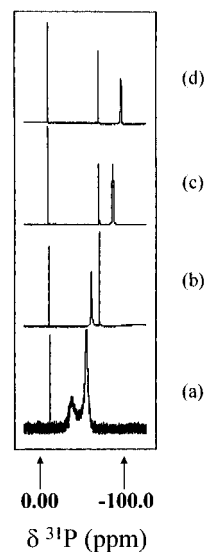


Figure 6. ³¹P NMR of [PdCl(PTA)₃]Cl with increasing amounts of added PTA: (a) 0 equiv excess; (b) 2 equiv excess; (c) 5 equiv excess; (d) 8 equiv excess.

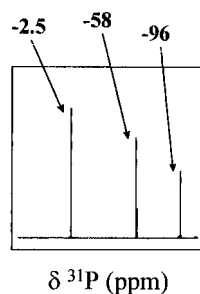


Figure 7. Final ³¹P NMR spectrum of [PdCl(PTA)₃]Cl with excess PTA.

appears to proceed by initial formation of PdCl₂(PTA)₂ with subsequent production of PdCl(PTA)₃⁺. Efforts to conclusively identify this latter salt by X-ray crystallography are ongoing in our laboratories.

Synthesis of *cis*-PtCl₂(PTA)₂ and Solid-State Structure of [*cis*-PtCl₂(PTAH)₂]Cl₂. Complex **7**, *cis*-PtCl₂(PTA)₂, was synthesized by the slow addition of an aqueous solution of K₂PtCl₄ to a boiling solution of PTA (3.6 equiv) in 95% ethanol. The initially milky orange reaction solution lightened to a yellow-orange color during the 2 h heating period. The solid resulting after solvent removal was washed several times with ethanol and ether to provide an off-white powder, isolated in 52% yield. The ³¹P NMR spectrum of **7** exhibited a singlet at –51.0 ppm with platinum satellites having a *J*_{Pt–P} of 3350 Hz.

Crystals of the protonated form of **7** were obtained from an 0.10 M HCl solution. Crystallographic data and data collection parameters for **7** determined at 193 K are found in Table 1. A thermal ellipsoid view of **7** is shown in Figure 8 along with the atom-numbering scheme. The pertinent bond distances and bond angles are listed in Table 7. The geometry about the Pt(II) center in **7** is a slightly distorted square plane with two *cis* chloride ligands and two *cis* phosphine ligands. The Cl–Pt–Cl angle is compressed to 86.2°, while the P–Pt–P angle is expanded to 94.3°. This is very similar to those reported for *cis*-[PtCl₂(PMe₃)₂] Cl–Pt–Cl 87.7°; P–Pt–P 96.2°²⁸ as well as the previously described palladium analog. This expansion, probably due to steric repulsion between the two phosphine ligands, is less than that reported for PMe₃, as can be anticipated

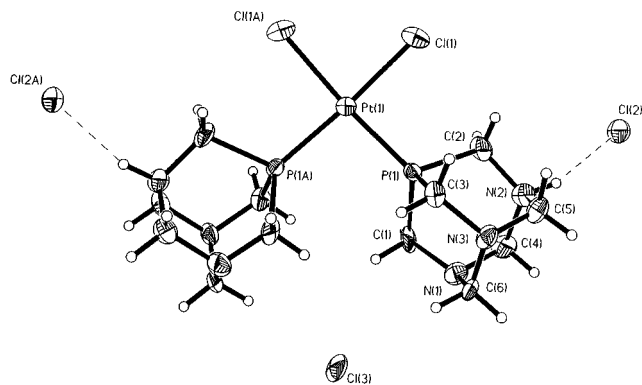


Figure 8. Thermal ellipsoid drawing of *cis*-[PtCl₂(PTAH)₂]Cl₂, with atom-numbering scheme.

Table 7. Selected Bond Lengths (Å)^a and Bond Angles (deg)^a for *cis*-[PtCl₂(PTAH)₂]Cl₂

Pt(1)–Cl(1)	2.358(5)	N(1)–C(6)	1.50
Pt(1)–Cl(1A)	2.358(5)	N(2)–C(2)	1.51
Pt(1)–P(1)	2.218(5)	N(2)–C(4)	1.53
Pt(1)–P(1A)	2.219(5)	N(2)–C(5)	1.50
N(1)–C(1)	1.42	N(3)–C(3)	1.52
N(1)–C(4)	1.48	N(3)–C(5)	1.44
Cl(1)–Pt(1)–P(1)	89.9(2)	Cl(1A)–Pt(1)–P(1A)	89.9(2)
Cl(1)–Pt(1)–Cl(1A)	86.2(2)	P(1)–Pt(1)–P(1A)	94.3
Cl(1)–Pt(1)–P(1A)	173.8(2)	P(1)–Pt(1)–Cl(1A)	173.8(2)

^a Estimated standard deviations are given in parentheses.

from their cone angles (102° PTA; 118° PMe₃).²⁰ The bond lengths are similar but slightly shorter than those of the PMe₃ analog (Pt–P 2.218 Å, Pt–Cl 2.358 Å for **7**; Pt–P 2.247 Å, Pt–Cl 2.376 Å for *cis*-PtCl₂(PMe₃)₂).²⁴ There is an extensive pattern of hydrogen bonding and electrostatic interactions involving water, PTA, and HCl (Figure 9). There are two symmetry-related hydrogen bonds (Cl–N 3.043 Å) that link the molecules into two-dimensional chains perpendicular to the *c* axis. This is very similar to the hydrogen bonding reported for Pd{P(CH₂OH)₃}₄.^{5a}

Conclusions

The water-soluble nitrosyl derivative of zero-valent nickel-containing PTA has been synthesized in good yield from the reduction of Ni(NO₃)₂ in the presence of NaNO₂ and PTA. X-ray crystallography and infrared spectroscopy show the complex to contain a near linear nitrosyl linkage as indicated by a ∠Ni–N–O of 171.5(4)° and a $\nu(\text{NO})$ value of 1830 cm⁻¹. In general, the coordination chemistry of the PTA ligand with the group 10 metals bears a close parallel to that of other basic, sterically nonencumbering phosphine ligands such as PMe₃ with the added property of facilitating water-solubility in both neutral and acidic aqueous media. That is, the M(PTA)₄ (M = Ni, Pd, Pt) derivatives are all slightly distorted tetrahedra which do not undergo facile phosphine dissociation in solution. Furthermore, the MCl₂(PTA)₂ (M = Pd, Pt) derivatives exhibit a close resemblance to their PMe₃ analogs. It should as well be pointed out that these M(PTA)₄ derivatives are protonated exclusively

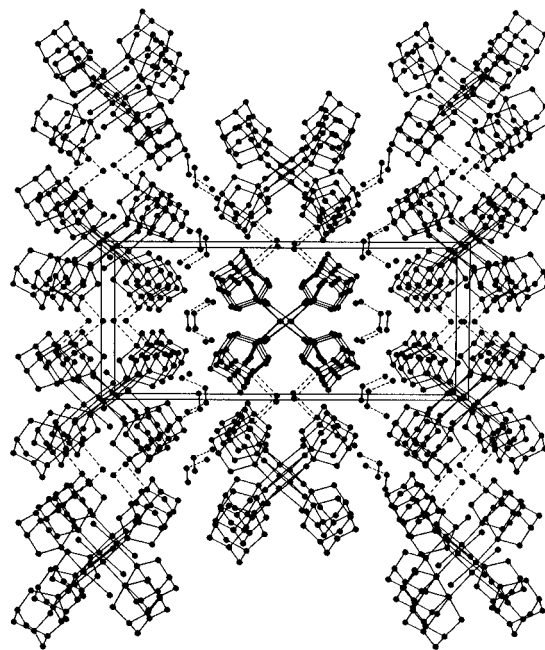


Figure 9. Network of hydrogen bonding and electrostatic interactions in crystal structures of *cis*-[PtCl₂(PTAH)₂]Cl₂·2H₂O involving water, PTA, and HCl.

Table 8. Chemical Shifts for PTA and Complexes of PTA Both Protonated and Nonprotonated

complex (nonprotonated)	³¹ P NMR shift (ppm)	complex (protonated) ^a	³¹ P NMR shift (ppm)
PTA	–96.0	PTAH ⁺	–90.5
Pt(PTA) ₄	–74.5	Pt(PTAH ⁺) ₄	–69.1
Pd(PTA) ₄	–58.7	Pd(PTAH ⁺) ₄	–54.2
Ni(PTA) ₄	–45.7	Ni(PTAH ⁺) ₄	–41.9

^a These contain chloride counterions.

at one nitrogen atom of the PTA ligand by HCl, with no products of oxidative addition such as M(PTA)₂(H)Cl being formed. This protonation process is unambiguously identified by both X-ray crystallography and ³¹P NMR spectroscopy (Table 8). Finally, the PTA ligand has the added advantage of being highly resistant to oxidation. Hence, these group 10 water-soluble phosphine complexes, much like the previously reported P(CH₂OH)₃ derivatives,⁵ afford opportunities for serving as catalysts or catalyst precursors for a large variety of reactions catalyzed by organometallic complexes.

Acknowledgment. The financial support of this research by the U.S. National Science Foundation (Grants CHE91-19737, CHE96-15866, and INT93-13951), Robert A. Welch Foundation, Hungarian National Research Foundation (Grant OTKA T016697), and Hungarian Ministry of Culture and Education (Grant 171/95) is greatly appreciated.

Supporting Information Available: X-ray crystallographic files in CIF format, for complexes **1a–4**, **6**, and **7** are available on the Internet only. Access information is given on any current masthead page.

IC970238X